



# Theoretical study of the influence of vacancies in the magnetic stability of V-, Cr-, and Mn-doped $\text{SnO}_2$

Pablo D. Borges<sup>a</sup>, Luisa M.R. Scolfaro<sup>b,\*</sup>, Horácio W. Leite Alves<sup>c</sup>, Eronides F. da Silva Jr.<sup>d</sup>, Lucy V.C. Assali<sup>e</sup>

<sup>a</sup> Inst. de Ciências Exatas e Tec., Universidade Federal de Viçosa, 38810-000 Rio Paranaíba, MG, Brazil

<sup>b</sup> Department of Physics, Texas State University, San Marcos 78666, TX, USA

<sup>c</sup> Universidade Federal de São João Del Rei, CP 110, 36301-160 São João Del Rei, MG, Brazil

<sup>d</sup> Departamento de Física, Universidade Federal de Pernambuco, 50670-901 Recife, PE, Brazil

<sup>e</sup> Instituto de Física, Universidade de São Paulo, 05315-970 São Paulo, SP, Brazil

## ARTICLE INFO

### Article history:

Received 29 September 2011

Received in revised form 8 August 2012

Accepted 11 August 2012

Available online 31 August 2012

### Keywords:

Dilute magnetic semiconductor

Magnetic metastability

Spintronics

Tin dioxide

Spin-crossover

## ABSTRACT

In this work we study, theoretically, the magnetic properties of transition metals (TMs)-doped  $\text{SnO}_2$  (with  $\text{TM} = \text{V, Cr, and Mn}$ ) in a diluted magnetic oxide configuration, focusing in particular in the role played by the presence of O vacancies,  $V_O$ , nearby the TM. We present the results of first-principles electronic structure calculations of  $\text{Sn}_{0.96}\text{TM}_{0.04}\text{O}_2$  and  $\text{Sn}_{0.96}\text{TM}_{0.04}\text{O}_{1.98}(V_O)_{0.02}$  alloys. The calculated total energy as a function of the total magnetic moment per cell shows a magnetic metastability, corresponding to a high-spin (HS) ground state, respectively, with 2 and 3  $\mu_B$ /cell, for Cr and Mn, and a metastable low-spin (LS) state, with 0 (Cr) and 1 (Mn)  $\mu_B$ /cell. For vanadium, only a state with 1  $\mu_B$ /cell was found. The spin-crossover energy ( $E_{SCO}$ ) from the LS to the HS is 114 meV for Cr and 42 meV for Mn. By creating O vacancies close to the TM site, we show that the metastability and  $E_{SCO}$  change. For chromium, a new HS state appears (4  $\mu_B$ /cell), with an energy barrier of 32 meV relative to the 2  $\mu_B$ /cell state. For manganese, the metastable LS state of 1  $\mu_B$ /cell disappears, while for vanadium the HS state of 1  $\mu_B$ /cell remains. In all cases, the ground state corresponds to the expected HS. These findings suggest that these materials may be used in applications that require different magnetization states.

© 2012 Elsevier B.V. All rights reserved.

## 1. Introduction

Recently tin dioxide ( $\text{SnO}_2$ ) doped with transition metals (TMs), has been extensively investigated due to the resulting important magnetic properties [1–6]. In particular, ferromagnetic (FM) behavior has been observed at room temperature in Cr-doped  $\text{SnO}_2$  diluted magnetic oxide (DMO) systems [7–9], indicating the potential of such systems for spintronic applications. It has also been observed that the presence of oxygen vacancies appears to be required for producing ferromagnetism in DMO, such as, e.g., in Co- and Fe-doped  $\text{ZnO}$  [10–13], in Co-doped  $\text{TiO}_2$  [14,15], in Fe- and Co-doping in  $\text{In}_2\text{O}_3$  [16,17] and in Co- and Cr-doped  $\text{SnO}_2$  [7,18,19]. A theoretical model proposed by Coey et al. to interpret the ferromagnetism in these semiconducting oxides requires the existence of oxygen vacancies in close proximity to TM sites in order to maintain the charge neutrality [20]. For TM-doped  $\text{SnO}_2$  nanoparticles, the FM behavior is limited by a maximum doping concentration  $x_L$  which has a strong relation with structural changes revealed from

X-ray diffraction measurements [7]. For example, the presence of oxygen vacancies in the  $\text{Sn}_{1-x}\text{Cr}_x\text{O}_2$  samples, in which the Cr concentrations  $x$  varies from 0 to 10% has been detected by electron paramagnetic resonance experiments [19]. The literature contains many efforts aimed at the characterization and understanding of the mechanisms involved in the FM behavior observed in such systems. However, no theoretical models based on rigorous ab initio electronic structure calculations have been published that establish unambiguously the roles played by TMs and by TMs with an oxygen vacancy nearby in  $\text{SnO}_2$  [21].

In this work, we study the magnetic metastability and electronic properties of  $\text{Sn}_{1-x}\text{TM}_x\text{O}_2$  ( $\text{TM} = \text{V, Cr, Mn}$ ) DMO alloys, for  $x = 0.04$ , i.e.,  $\text{Sn}_{0.96}\text{TM}_{0.04}\text{O}_2$  alloys, through ab initio electronic structure calculations performed within the spin density functional theory. We have chosen the concentration of  $x = 0.04$  for the calculations since it corresponds to a typical experimental value (in the range which most of the experimental work has been done) and the alloy can be easily simulated by a reasonable size supercell. The magnetic metastability has been recently investigated in other systems like GaN:TM [22]. Additionally, we also study the influence of an oxygen vacancy ( $V_O$ ) nearest neighbor to the TM atom in the alloys,  $\text{Sn}_{1-x}\text{TM}_x\text{O}_{2-y}(V_O)_y$  systems, with  $x = 0.04$  and  $y = 0.02$ ,

\* Corresponding author. Tel.: +51 2458610.

E-mail addresses: [lscolfaro@txstate.edu](mailto:lscolfaro@txstate.edu), [ls61@txstate.edu](mailto:ls61@txstate.edu) (L.M.R. Scolfaro).

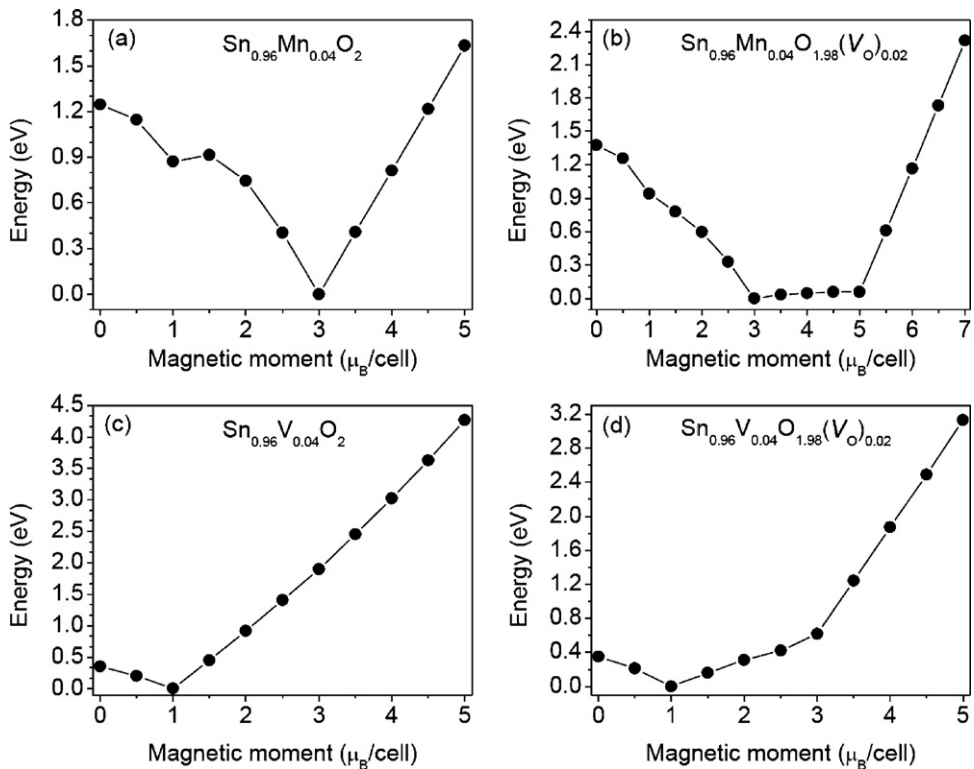


**Fig. 1.** Total energy vs. magnetic moment per cell for (a)  $\text{Sn}_{0.96}\text{Mn}_{0.04}\text{O}_2$ , (b)  $\text{Sn}_{0.96}\text{Mn}_{0.04}\text{O}_{1.98}(\text{V}_\text{O})_{0.02}$ , (c)  $\text{Sn}_{0.96}\text{V}_{0.04}\text{O}_2$  and (d)  $\text{Sn}_{0.96}\text{V}_{0.04}\text{O}_{1.98}(\text{V}_\text{O})_{0.02}$ . The total energy of the high spin ground state is set to zero.

i.e.,  $\text{Sn}_{0.96}\text{TM}_{0.04}\text{O}_{0.98}(\text{V}_\text{O})_{0.02}$  alloys, and its consequences for the magnetic behavior of TM-doped  $\text{SnO}_2$ .

## 2. Calculation method

All calculations were based on the spin density functional theory. We employed the Projector Augmented Wave method implemented in the Vienna Ab-initio Simulation Package (VASP-PAW) [23,24]. The exchange-correlation potential used was the generalized gradient approximation in the Perdew, Burke, and Ernzerhof (GGA-PBE) [25] approach. The method has been

previously used to study the structural and electronic properties of bulk rutile  $\text{SnO}_2$  [26]. The valence electronic distributions for the PAWs representing the atoms were Sn –  $4d^{10} 5s^2 5p^2$ , O –  $2s^2 2p^6$ , V –  $3d^3 4s^2$ , Cr –  $3d^5 4s^1$ , and Mn –  $3d^5 4s^2$ , and scalar relativistic effects were taken into account. To describe the alloys, we used a 72-atoms supercell (24 Sn and 48 O atoms) and a  $4 \times 4 \times 4$  Monkhorst–Pack mesh k-points for integration in the Brillouin Zone. All the calculations were done with a 490 eV energy cutoff in the plane-wave expansions and the systems were fully relaxed until the residual forces on the ions were less than 10 meV/Å.

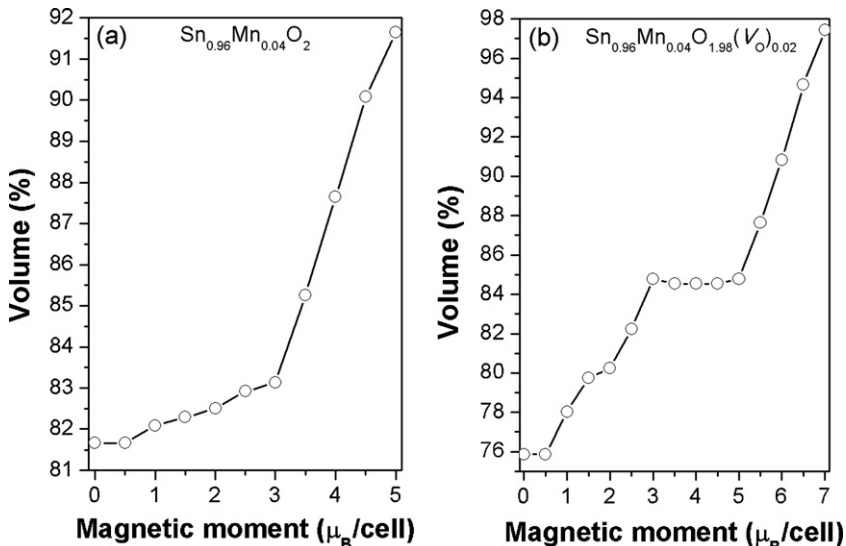


**Fig. 2.** Relative volume (%) around manganese impurity vs. magnetic moment per cell for (a)  $\text{Sn}_{0.96}\text{Mn}_{0.04}\text{O}_2$  and (b)  $\text{Sn}_{0.96}\text{Mn}_{0.04}\text{O}_{1.98}(\text{V}_\text{O})_{0.02}$ .

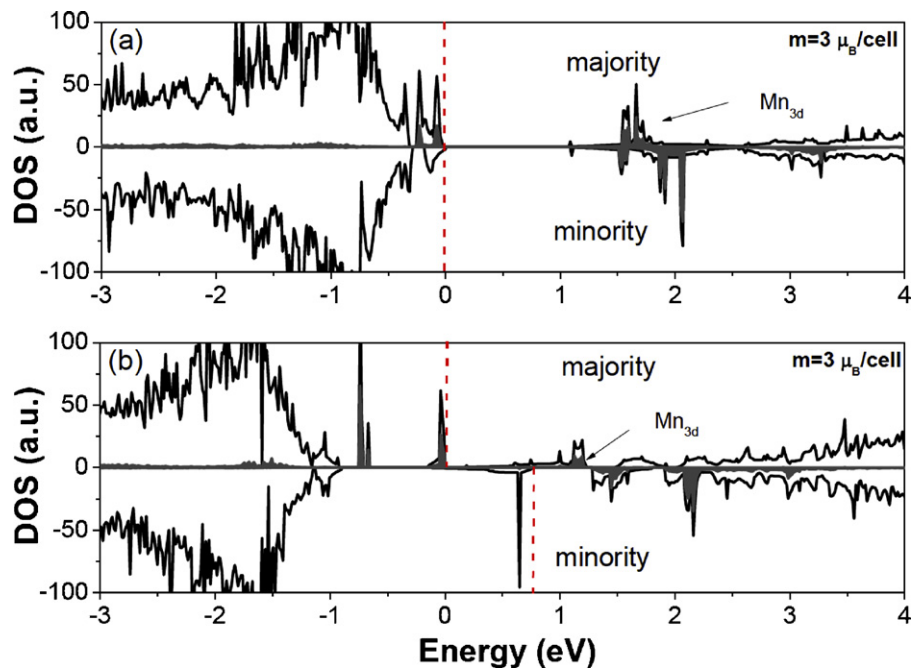


**Fig. 3.** The total (black lines) and projected (gray shaded areas) density of states of the Mn 3d derived states for the majority and minority spins for the magnetic moment equal to  $3 \mu_B/\text{cell}$  are shown for (a)  $\text{Sn}_{0.96}\text{Mn}_{0.04}\text{O}_2$  and (b)  $\text{Sn}_{0.96}\text{Mn}_{0.04}\text{O}_{1.98}(\text{V}_0)_{0.02}$ . The vertical (dashed) line corresponds to the highest occupied energy level for the majority and minority spin.

### 3. Results and discussion

We studied the systems  $\text{Sn}_{0.96}\text{TM}_{0.04}\text{O}_2$  and the  $\text{Sn}_{0.96}\text{TM}_{0.04}\text{O}_{1.98}(\text{V}_0)_{0.02}$  with the oxygen vacancy as the TM nearest neighbor. In both cases a single tin atom was substituted with a TM atom in the 72-atoms supercell, simulating the  $x=0.04$  impurity concentration. For all cases the total energy was calculated for several magnetic moment values.

It was recently shown by us [27] that when a Sn atom is replaced by a chromium atom in  $\text{SnO}_2$ , a high spin (HS) ground state with a magnetic moment  $m=2 \mu_B/\text{cell}$  and a low spin state (LS) with a magnetic moment  $m=0 \mu_B/\text{cell}$  are seen. For this case a spin crossover becomes possible with an energy barrier of 114 meV calculated for the transition from  $m=0 \mu_B/\text{cell}$  to  $m=2 \mu_B/\text{cell}$ . When an oxygen vacancy (out of the six first-neighbors of Cr) is considered, the total behavior of the energy vs. the magnetic moment per cell showed the appearance of a second HS configuration, with magnetic moment  $m=4 \mu_B/\text{cell}$ , and an energy barrier of 32 meV relative to the  $2 \mu_B/\text{cell}$  state was found. The ground state, however, remains as the  $2 \mu_B/\text{cell}$  magnetic moment HS state. The energy barrier for the  $m=0 \mu_B/\text{cell}$  to  $m=2 \mu_B/\text{cell}$  transition was reduced to 27 meV. Comparing the same transition for the DMO without the vacancy of 114 meV, a drastic reduction by about 75% is observed.

We show here that if a single Sn atom is substituted with a manganese atom, the magnetic metastability seen for Cr can also occur. Fig. 1(a) and (b) shows the total energy behavior for the  $\text{Sn}_{0.96}\text{Mn}_{0.04}\text{O}_2$  and  $\text{Sn}_{0.96}\text{Mn}_{0.04}\text{O}_{1.98}(\text{V}_0)_{0.02}$  alloys, respectively. A HS ground state with a magnetic moment  $m=3 \mu_B/\text{cell}$  and a LS state with a magnetic moment  $m=1 \mu_B/\text{cell}$  were observed for the system without the oxygen vacancy, with an energy barrier of 42 meV for the transition from  $m=1 \mu_B/\text{cell}$  to  $m=3 \mu_B/\text{cell}$ . When the oxygen vacancy is considered  $m=1 \mu_B/\text{cell}$  is no longer a metastable state, however new states between  $3 < m \leq 5$  appear with energy values very close to the ground state at  $m=3 \mu_B/\text{cell}$  and an almost flat region between  $m=3 \mu_B/\text{cell}$  and  $m=5 \mu_B/\text{cell}$  is seen.

Fig. 1(c) and (d) shows the total energy vs. magnetic moment for  $\text{Sn}_{0.96}\text{V}_{0.04}\text{O}_2$  and  $\text{Sn}_{0.96}\text{V}_{0.04}\text{O}_{1.98}(\text{V}_0)_{0.02}$  alloys, respectively.

The ground state is at  $m=1 \mu_B/\text{cell}$  independently of the presence or absence of an oxygen vacancy. For the case V-doped  $\text{SnO}_2$  the magnetic metastability is not observed and also the presence of the oxygen vacancy did not provide an increase of magnetic metastable states, as in the case of the chromium and manganese impurities.

We can try to understand the values of  $m$  observed by analyzing the TM charges states and the neighbor atoms around it. For the  $\text{Sn}_{0.96}\text{Cr}_{0.04}\text{O}_2$  alloy the  $\text{Cr}^{4+}$  ( $3d^2$ ) impurity replacing  $\text{Sn}^{4+}$  allows the magnetic states  $m=0$  and  $2 \mu_B$ . In this case the neighborhood does not contribute to the magnetization of the system. When an oxygen vacancy is taken into account, the impurity state changes from  $\text{Cr}^{4+}$  to  $\text{Cr}^{3+}$  ( $3d^3$ ) and the neighboring atoms contribute for the magnetic moment. Three spin up electrons from Cr plus one spin-down electron arising from the neighboring atoms allow for the metastable state with  $m=2 \mu_B$ , while three spin-up electrons from Cr plus one spin-up electron coming from the neighboring atoms allow for the metastable state  $m=4 \mu_B$ . These results are in agreement with the experimental data. Misra et al. [19] have shown that the EPR spectra of  $\text{Cr}^{3+}$  doping ions in sample of  $\text{SnO}_2$  nanoparticles exhibit a ferromagnetically ordered component due to oxygen vacancies.

Likewise, the  $\text{Mn}^{4+}$  ( $3d^3$ ) impurity replacing  $\text{Sn}^{4+}$  allows the magnetic states  $m=1$  and  $3 \mu_B/\text{cell}$  without the need of electrons coming from the neighborhood. If an oxygen vacancy is present the TM state changes from  $\text{Mn}^{4+}$  to  $\text{Mn}^{3+}$  ( $3d^4$ ). The magnetic moment value equal to  $3 \mu_B/\text{cell}$  is a result of the four manganese spin-up electrons and one spin-down electron provided by the neighbor atoms. X-ray photoelectron spectroscopy studies have confirmed the incorporation of  $\text{Mn}^{3+}$  cations into rutile  $\text{SnO}_2$  lattice [28,29]. For vanadium doping in tin dioxide the EPR and XPS studies [30,31] revealed the existence of  $\text{V}^{4+}$  ions incorporated in  $\text{SnO}_2$ .

As noted for the chromium impurity, for the manganese and vanadium impurities we observe a relationship between the structural modification around the TM atom, due to the electronic and ionic relaxations, and the occurrence of the magnetic metastability. If we consider a spherical volume involving the TM whose radius is an average distance between the TM and the six oxygen first neighbors, our calculations showed that, after full relaxation the

corresponding volume is reduced. For Cr the volume is reduced by about 16% for the HS state ( $2 \mu_B/\text{cell}$ ) and by 17.5% for the LS state ( $0 \mu_B/\text{cell}$ ). Considering the oxygen vacancy, for the HS states ( $2 \mu_B/\text{cell}$  and  $4 \mu_B/\text{cell}$ ) the volume reductions, after full relaxed calculations, were 20% and 22%, respectively, while for the LS state ( $0 \mu_B/\text{cell}$ ) it was 31%. For LS configurations the presence of a missing oxygen atom allows greater relaxations which reduce the total energy of the system lowering the energy barrier for the crossover. As shown in Fig. 2(a) for Mn the volume is reduced by about 17% for the HS state ( $3 \mu_B/\text{cell}$ ) and by 18.5% for the LS state ( $1 \mu_B/\text{cell}$ ). If the oxygen vacancy is present the volume around the Mn impurity is reduced by about 15% for the magnetic moment between  $3 \mu_B/\text{cell}$  and  $5 \mu_B/\text{cell}$  forming an almost flat region.

The observed magnetic metastability in the DMOs studied here is attributed to a structural modification (relaxation) around the TM impurity. The presence or absence of magnetism in this case is determined by a competition between intra-atomic exchange interactions and inter-atomic electronic motion due to the crystalline field [32]. Therefore, the occurrence of the LS and HS states depends on the effective balance between these two interaction fields. The LS state occurs when the crystal field splitting is larger than the intra-atomic exchange splitting (lowest volume), and otherwise, the HS state is the ground state (highest volume).

The total (TDOS) and projected (PDOS) density of states of the Mn 3d orbital are shown in Fig. 3(a) and (b) for the cases  $\text{Sn}_{0.96}\text{Mn}_{0.04}\text{O}_2$  and  $\text{Sn}_{0.96}\text{Mn}_{0.04}\text{O}_{1.98}(\text{V}_0)_{0.02}$  alloys, respectively. The vertical lines represent the highest occupied energy values for the majority and minority spin. For both cases the manganese 3d states are found to lie in the gap region and, showing a half-metallic behavior.

#### 4. Conclusions

The magnetic and electronic properties of chromium, manganese and vanadium as an impurity in a DMO configuration in rutile tin dioxide,  $(\text{Sn}_{0.96}\text{TM}_{0.04}\text{O}_2)$ , were studied using ab initio calculations performed within the spin-density functional theory. A magnetic metastability was observed. Energy barriers were obtained for the spin crossover between the  $m=0 \mu_B/\text{cell}$  and  $m=2 \mu_B/\text{cell}$  states in  $\text{Sn}_{0.96}\text{Cr}_{0.04}\text{O}_2$  and  $m=1 \mu_B/\text{cell}$  and  $m=3 \mu_B/\text{cell}$  states in  $\text{Sn}_{0.96}\text{Mn}_{0.04}\text{O}_2$ . For vanadium the magnetic metastability was not observed. When an oxygen vacancy is considered as one of the six first-neighbors to the Cr and Mn impurities in these alloys (the  $\text{Sn}_{0.96}\text{Cr}_{0.04}\text{O}_{1.98}(\text{V}_0)_{0.02}$  and  $\text{Sn}_{0.96}\text{Mn}_{0.04}\text{O}_{1.98}(\text{V}_0)_{0.02}$ ) a considerable modification is observed in the magnetic metastability behavior, with the occurrence of a second high-spin configuration with magnetic moment  $m=4 \mu_B/\text{cell}$  for the chromium impurity with significantly lower energy barriers, 27 meV, for the system to flip from the low-spin to the high-spin state, and the disappearance of the state with  $m=1 \mu_B/\text{cell}$  for the manganese impurity. This behavior

is attributed to the relative contributions of the intra-atomic exchange interactions effects and the inter-atomic electron motion effects due to the crystalline field which are responsible for the relaxations around the TM impurities.

#### Acknowledgements

This work was partially supported by the Brazilian funding agencies FAPEMIG, FAPESP, CAPES, and CNPq, and by the Materials Science, Engineering and Commercialization Program at Texas State University in San Marcos.

#### References

- [1] X. Mathew, et al., J. Appl. Phys. 100 (2006) 073907.
- [2] H. Kimura, et al., Appl. Phys. Lett. 80 (2002) 94.
- [3] W. Wang, et al., J. Appl. Phys. 99 (2006) 08M115.
- [4] S.B. Ogale, et al., Phys. Rev. Lett. 91 (2003) 077205.
- [5] C.E. Rodriguez Torres, J. Magn. Magn. Mater. 316 (2007) e219.
- [6] M. Batzill, et al., Thin Solid Films 484 (2005) 132.
- [7] C. Van Komen, A. Thurber, K.M. Reddy, J. Hays, A. Punnoose, J. Appl. Phys. 103 (2008) 07D141.
- [8] N.H. Hong, J. Sakai, W. Prellier, A. Hassini, J. Phys.: Condens. Matter 17 (2005) 1697.
- [9] C.B. Fitzgerald, et al., Phys. Rev. B 74 (2006) 115307.
- [10] A. Fouchet, W. Prellier, P. Padhan, Ch. Simon, B. Mercey, V.N. Kulkarni, T. Venkatesan, J. Appl. Phys. 95 (2004) 7187.
- [11] B. Martineza, F. Sandiumengea, Ll. Balcells, J. Fontcubertaa, F. Sibieudeb, C. Montyb, J. Magn. Magn. Mater. 290–291 (2005) 168.
- [12] R.K. Singhal, et al., J. Alloys Compd. 496 (2010) 324.
- [13] A. Samariya, R.K. Singhal, S. Kumar, Y.T. Xing, M. Alzamora, S.N. Dolia, U.P. Deshpande, T. Shripathi, E.B. Saitovitch, Mater. Chem. Phys. 123 (2010) 678.
- [14] R.K. Singhal, et al., Solid State Commun. 150 (2010) 1154.
- [15] R.K. Singhal, et al., J. Appl. Phys. 107 (2010) 113916.
- [16] A. Samariya, R.K. Singhal, S. Kumar, Y.T. Xing, S.C. Sharma, P. Kumari, D.C. Jain, S.N. Dolia, U.P. Deshpande, T. Shripathi, E. Saitovitch, Appl. Surf. Sci. 257 (2010) 585.
- [17] R.K. Singhal, A. Samariya, S. Kumar, S.C. Sharma, Y.T. Xing, U.P. Deshpande, T. Shripathi, E. Saitovitch, Appl. Surf. Sci. 257 (2010) 1053.
- [18] J. Hays, A. Punnoose, R. Baldner, M.H. Engelhard, J. Peloquin, K.M. Reddy, Phys. Rev. B 72 (2005) 075203.
- [19] S.K. Misra, S.I. Andronenko, S. Rao, S.V. Bhat, C.V. Komen, A. Punnoose, J. Appl. Phys. 105 (2009) 07C514.
- [20] J.M.D. Coey, et al., Nat. Mater. 4 (2005) 173.
- [21] For a recent review see e.g., S.B. Ogale, Adv. Mater. 22 (2010) 3125, and references therein.
- [22] X.Y. Cui, et al., Phys. Rev. Lett. 97 (2006) 016402.
- [23] G. Kresse, J. Furthmüller, Comput. Mater. Sci. 6 (1996) 15.
- [24] G. Kresse, J. Furthmüller, Phys. Rev. B 54 (1996) 11169.
- [25] J.P. Perdew, K. Burke, M. Ernzerhof, Phys. Rev. Lett. 77 (1996) 3865.
- [26] P.D. Borges, L.M.R. Scolfaro, H.W. Leite Alves, E.F. da Silva Jr., Theor. Chem. Acc. 126 (2010) 39.
- [27] P.D. Borges, L.M.R. Scolfaro, H.W. Alves, E.F. da Silva Jr., L.V.C. Assali, Mater. Sci. Eng. B 176 (2011) 1378.
- [28] Z.M. Tian, S.L. Yuan, J.H. He, P. Li, S.Q. Zhang, C.H. Wang, Y.Q. Wang, S.Y. Yin, L. Liu, J. Alloys Compd. 466 (2008) 26.
- [29] Y. Xiao, S. Ge, L. Xi, Y. Zuo, X. Zhou, B. Zhang, L. Zhang, C. Li, X. Han, Z. Wen, Appl. Surf. Sci. 254 (2008) 7459.
- [30] R.S. Ningthoujam, D. Lahiri, V. Sudarsan, H.K. Poswal, S.K. Kulshreshtha, S.M. Sharma, B. Bhushan, M.D. Sastry, Mater. Res. Bull. 42 (2007) 1293.
- [31] L. Zhang, S. Ge, Y. Zuo, X. Zhou, Y. Xiao, S. Yan, X. Han, Z. Wen, J. Appl. Phys. 104 (2008) 123909.
- [32] V.L. Moruzzi, Phys. Rev. Lett. 57 (1986) 2211.